10th IMEKO TC14 Symposium on
Laser Metrology for Precision Measurement and Inspection in Industry
Braunschweig, GERMANY, 2011, September 12-14

Contouring of Rough Surfaces by Digital Holography

Ichirou Yamaguchi, Toyo Seiki Seisakusho, 1-2-6 Funado, Itabashi-ku, Tokyo, Japan

Abstract

Measurement of surface shape of diffusely reflecting objects by phase shifting digital holography is described. After basic principles and an experimental result are briefly explained, a digital simulation algorithm is presented that delivers 2-dimensional distributions of the reconstructed images and contours for general object and hologram recording conditions.

Keywords:

Digital holography, shape and deformation measurement, speckle suppression

Introduction

In industry it is strongly required to measure surface shape of various objects accurately and quickly. Optical methods fulfill these requirements well because of their noncontacting and whole-field capabilities that need no mechanical scanning. They can be classified into two categories depending on the coherence of light used.

Incoherent methods consist of triangulation, autofocusing, and pattern projection methods [1]. In these methods some markings such as a spot or line or a grating must be printed or projected on the surfaces. Either lateral shift or sharpness of these patterns are monitored to detect the longitudinal position of the markings that delivers surface height. For the whole field measurement phase distribution of a grating image is detected.

In coherent methods based on interferometry a laser light is employed to relate the sensitivity to laser wavelength. Compared with the incoherent methods the coherent methods such as holography achieve higher sensitivity and enable measurements of both surface shape and deformation with the same setup by detecting the phase change of the light diffusely reflected from the object due to changes of illumination and surface deformation, respectively.

Digital holography provides 3-d distributions of complex amplitude of coherent images of arbitrary objects leading to noncontacting and automatic measurements of shape and deformation of rough surfaces with simpler optical setups without imaging systems.

In this paper we describe the surface contouring methods using digital holography We also report a computer simulaton that can be applied to various cases encountered in practical applications with general optical, recording, and processing systems. We deal with the con-

touring using phase-shifting digital holography that allows larger measurement area than the off-axis method [2]. Surface contouring by phase-shifting digital holography was treated analytically on the basis of linear transmission of complex amplitude from an object to a hologram and an observation point [3]. However, this approach cannot be applied to the general circumstances with arbitrary surface roughness of an object and recording conditions of digital holograms, which can be treated numerically in the present analysis.

Principles and Experimental Results

Surface contouring by phase-shifting digital holography with dual wavelength method [4] is carried out by using the setup shown in Fig.1.

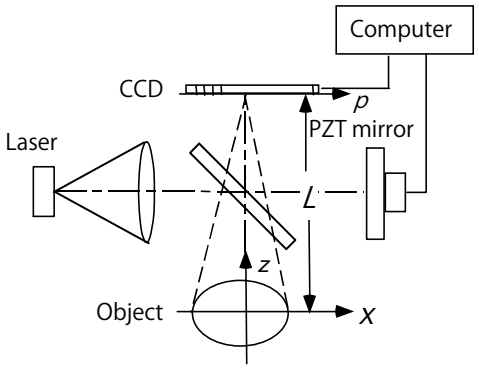

Fig.1: Setup for surface contouring by phase-shifting digital holography.

A laser beam is divided into two paths, a reference and an object, and recombined to generate an in-line hologram whose spatial frequency becomes lowest. A PZT mirror shifts the reference phase δ.

The hologram intensity is given by

$$I_H(p,q;\delta) = \left|U_R \exp(i\delta) + U_O(p,q)\right|^2 \qquad (1)$$

From three phase-shifted hologram we obtain the complex amplitude at the CCD plane such as

$$U_O = \left\{I_H(0) - I_H(\pi) + i\left[I_H(0) - 2I_H(\pi/2) + I_H(\pi)\right]\right\}/U_R^* \qquad (2)$$

where the coordinate variables (p,q) have been dropped for simplicity. The complex amplitude of the object wave at the plane located at the distance L-Z from the CCD is reconstructed by calculating the Fresnel transform of $U_O(p,q)$ as given by

$$U(X,Y,Z) = \iint U_O(p,q) \exp\left[-ik\frac{(X-p)^2+(Y-q)^2}{2(L-Z)}\right] dpdq \quad (3)$$

For surface contouring using dual wavelengths we record and reconstruct the object waves U_a and U_b, with wavelengths $\lambda_a=2\pi/k_a$ and $\lambda_b=2\pi/k_b$. Earlier we calculated the phase difference of the reconstructed waves corresponding to λ_a and λ_b.

In the new approach we derive the phase of the coherence factor, that is, the averaged conjugate product of complex amplitude at the object plane Z =0 as given by and becomes in the case of surface contouring using dual wavelengths [5]

$$\Phi(x,y) = \arg\langle U_a(x,y,0) U_b^*(x,y,0)\rangle = 2Kh(x,y) = 4\pi h(x,y)/\Lambda \quad (4)$$

where $h(x,y)$ is surface height and the $\Lambda = 2\pi/K = 2\pi/(k_a - k_b)$ is the synthetic wavelength. It is a unique advantage of digital holography that we can calculate this coherence factor directly instead of fringe detection and analysis in the conventional interferometry. This averaging realizes the suppression of the speckle noise that arises from the interference between lights scattered from different surface points. It is derived from the theoretical relationship for fringe formation from diffusely reflected light [6].

In experiments we used a laser diode of wavelength λ=657 nm and output power of 30 mW. Its wavelength shift of 0.508 nm was provided by mode-hop of the laser diode subject to change of injection current between 55 mA and 59 mA. Three phase-shifted holograms were recorded by a CCD having 512x512 pixels of the pitch equal to 12.92 x 12.87 μm^2 each before and after the wavelength shift. The video signal is A/D converted at 8 bits. The wavelength shift proved to be $\Delta\lambda=\lambda_b-\lambda_a$ 0.508±0.0038 nm from λ= 657.44 nm that resulted from the measurement over repetitions of 20 times switching of the injection current. This wavelength shift leads to the height sensitivity equal to $\Delta h = \Lambda/2 = \lambda^2/2\Delta\lambda$=424±3.0 μm. Therefore, the uncertainty of height is less than 1%. This wavelength change was accompanied by a change of output power, which does not affect the result, however, because of Eq.(4). Figure 2 shows the results from a pingpong ball whose diameter of 30 mm positioned at a distance of 327 mm from the CCD. The fine surface wrinkles might be attributed to internal reflection within the plastic skin.

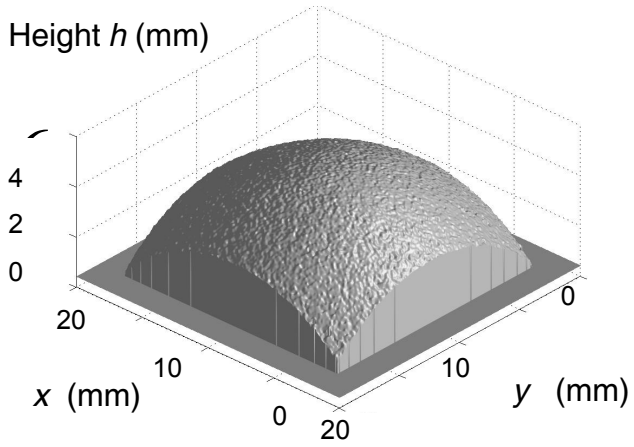

Fig. 2: Experimental result from a pingpong ball.

Basics of Computer Simulations

For evaluating the feasibility of the contouring method mentioned above and for investigating the effects of surface roughness, CCD specifications, and reconstruction conditions we conducted computer simulations. In order to visualize focusing effects and to reduce computation time we start from the two-dimensional coordinate system shown in Fig.3.

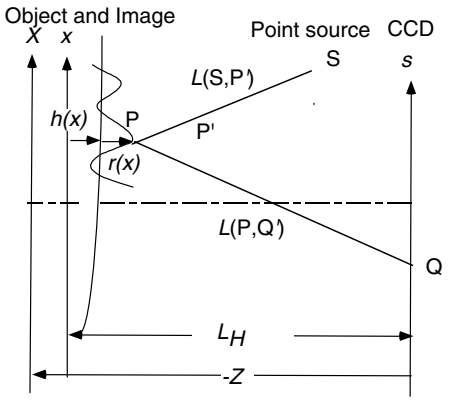

Fig. 3: Coordinate system used for simulation.

A diffuse object is illuminated by a point monochromatic source S with the wavelength λ. A rough surface is assumed to consist of point scatterers whose position is represented by P[*x*,*h(x)*+*r(x)*] where *h(x)* and *r(x)* mean the initial mean surface and the random roughness profile, respectively. The distribution of *r(x)* is represented by random numbers uniformly distributed between ($-r_m/2$, $r_m/2$) where r_m represents the maximum surface roughness. At the point Q on the hologram plane the complex amplitude of a spherical wave scattered from the

surface point associated with a sample point x_j at the object plane is added with macroscopic amplitude depending on both illumination and the surface reflectivity such as

$$U(s:\lambda)=\sum_{j=1}^{M}\sqrt{I_O(x_j)}\exp\left\{i(2\pi/\lambda)\left[L(S:P_j)+L(P_j:Q)\right]\right\} \tag{5}$$

where $I_o(x)$ is the macroscopic intensity distribution at the object and

$$L(A:B)=\sqrt{(x_A-x_B)^2+(z_A-z_B)^2} \tag{6}$$

is the distance between the points A(x_A,z_A) and B(x_B,z_B). At the CCD plane distant from the object by L_H the complex amplitude is combined with the reference beam having the complex amplitude $U_R=A_R e^{i\delta}$ to yield the intensity

$$I_H(s:\lambda:\delta)=\left|A_R\exp(i\delta)+U(s:\lambda)\right|^2 \tag{7}$$

Each pixel of the CCD with the pitch p, the width w, and the pixel number N delivers the output signal

$$S(m:\lambda:\delta)=\int_{(m-1)p}^{(m-1)p+w} I_H(s:\lambda:\delta)ds \quad (m=1\ \sim N) \tag{8}$$

In the case of three-steps algorithm the complex amplitude of the object wave is derived such as

$$\begin{aligned} U_O(m:\lambda)&=S(m:\lambda:0)-S(m:\lambda:\pi)\\ &\quad+i\left[S(m:\lambda:0)-2S(m:\lambda:\pi/2)+S(m:\lambda:\pi)\right] \end{aligned} \tag{9}$$

The image reconstruction is conducted by the angular spectrum method instead of the Fresnel transformation of Eq.(3). It is more appropriate here because of no limitation on the distance between the object and the reconstruction plane as well as the constant sample pitch of the reconstructed image equal to p.

For image reconstruction by the angular spectrum expansion we first calculate the Fourier transform $\hat{U}(m:a)$ of the above derived complex amplitude given by

$$\hat{U}_O(m:\lambda)=\sum_{n=1}^{N}U_O(n:\lambda)\exp(-i2\pi mn) \quad (10)$$

which leads to the complex amplitude at the plane *Z* from the object calculated as

$$U(n,Z:\lambda)=$$
$$\sum_{m=1}^{N}\hat{U}_O(m:\lambda)\exp\left[i2\pi\left(nm-(L_H-Z)\sqrt{\frac{1}{\lambda^2}-\left(\frac{m}{Np}\right)^2}\right)\right] \quad (11)$$

For surface contouring we calculate the complex coherence factor defined by an average of the conjugate product of the complex amplitudes before and after wavelength change over 2*J*+1 pixels on the reconstruction plane

$$\Gamma(n,Z)=\sum_{m=-J}^{J}U(n+m,Z:\lambda)U^*(n+m,Z:\lambda+\Delta\lambda) \quad (12)$$

We showed that the phase of the coherence factor is proportional to object displacement and that speckle noise is suppressed more efficiently by this algorithm.

Simulation Results for Marked Objects

We examined 3-dimensional imaging properties of the phase-shifting digital holography. We employed a cylindrical rough surface of the same diameter 30 mm used in the above experiment. The cross-section of the mean surface height is shown in Fig.4(a). First we assumed that on the surface dark lines are printed and that the macroscopic intensity reflection function is represented by the rectangular function as shown in Fig.4(b). The same function is also realized by illuminating the surface through a grid mask.

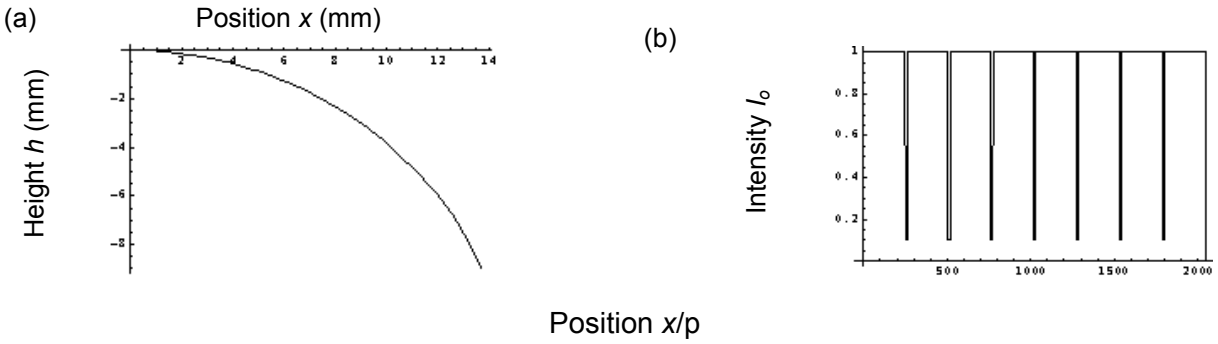

Fig. 4: Surface height (a) and reflection function (b) of the cylindrical object employed in the simulation.

The vertex of the surface is at a distance of 227 mm from the CCD of the pitch 5 μm and the number 2048. The beam width on the object is 15 mm. The wavelength is λ=660 nm. The maximum surface roughness is r_m=10 μm and the number of object points is M=2048.

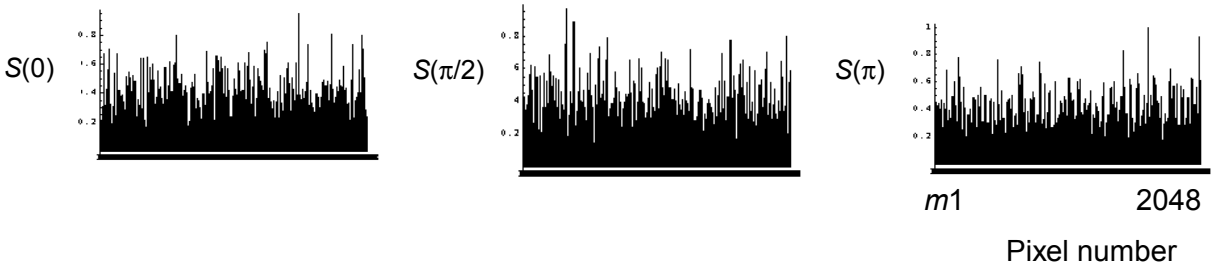

Fig. 5: CCD signals corresponding to three phase- shifted holograms.

The three phase-shifted holograms formed by the interference with a plane in-line reference beam delivers the CCD outputs shown in Fig.5. These signals exhibit speckled structures whose correlation length is proportional to the wavelength divided by the angular object size as seen from the CCD.

The amplitude and phase of the object wave that are derived from the CCD signals by means of Eq.(9) become as shown in Fig.6. They also exhibit speckled structures.

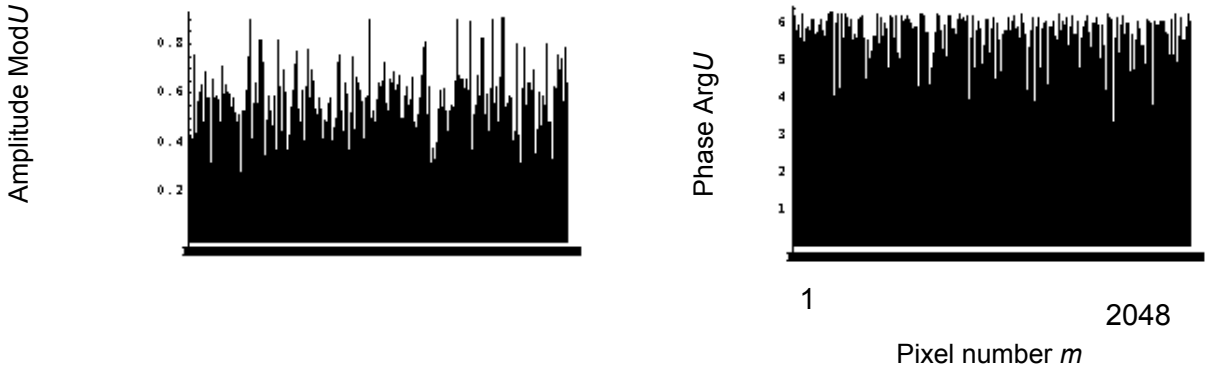

Fig. 6: Amplitude (a) and phase (b) of the object wave at the CCD plane.

The reconstructed image has a two-dimensional distribution of intensity as shown in Fig.7(a). The horizontal axis is along Z and the vertical axis is along X. The scales along each axis are 0.1 mm and p=6.7μm, respectively. The distribution of the target image is modulated by speckle and the dark region has the largest total area. If we only display the darkest region whose intensity is lower than 0.05% of the maximum intensity in the whole region by invert-

ing the intensity, we obtain the distribution of Fig.7(b) that does not exhibit all the target images whose axial position indicates the surface height. All the target images are not visible because the speckle noise has shaded some of the target images. We suppressed the speckle noise by smoothing the intensity over 3 pixels at each reconstruction plane with various values of *Z*.

The results are shown in Fig.8. The target positions can be seen more clearly because the dark bands and their darkest regions are displayed over the whole surface. Thus after smoothing the intensity we can see the images of dark marking more clearly and all the image positions can be identified. Centers of the dark bands might be estimated as the surface positions. Resolution of this method depends not only on the focal depth of the digital holographic system but also on the width and modulation of the markings. These dependences can be analyzed in detail by the present model.

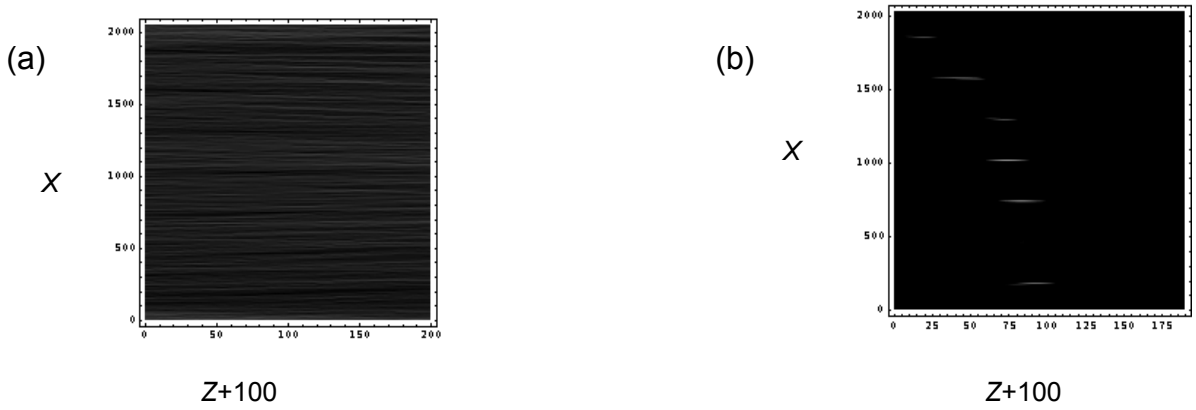

Fig. 7: (a) Cross-section of original reconstruction of the object with target lines.
(b) Display of the darkest region after the intensity reversal. *X*-scale=6.7 μm, *Z*-scale=0.1 mm

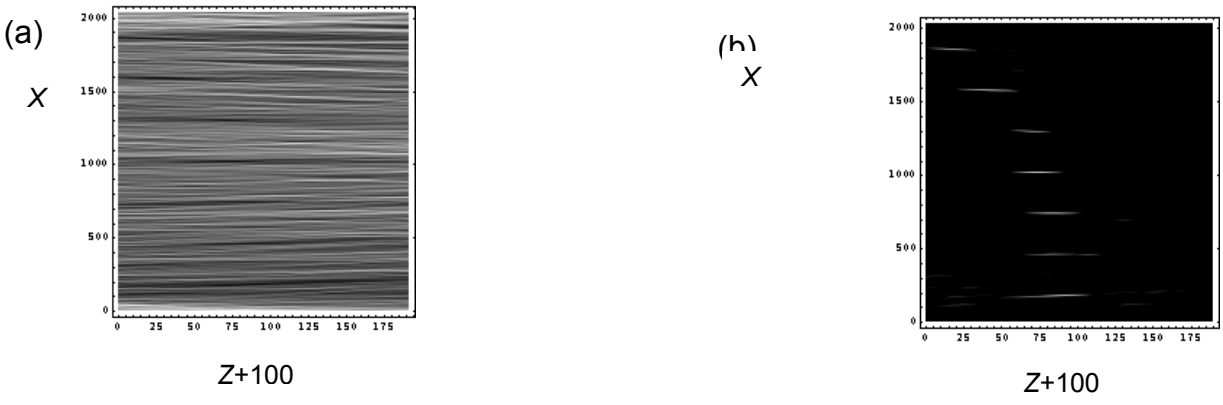

Fig. 8: Cross-section of the reconstructed intensity after smoothing (a) and its darkest region (b). *X*-scale=6.7 μm, *Z*-scale=0.1 mm

In a primitive examination the height resolution of this focusing method is estimated from the focal depth of the target image that is represented by

$$\Delta Z = \lambda\left(L_H / Np\right)^2 \qquad (13)$$

In the present condition it becomes ΔZ=0.18 mm that is less than 1/10 the depth of the above images. The most remarkable benefit of the present method might be that no mechanical scanning is necessary as in the conventional focal sensors.

Simulations for Dual Wavelength Contouring

We can improve the sensitivity of contouring by

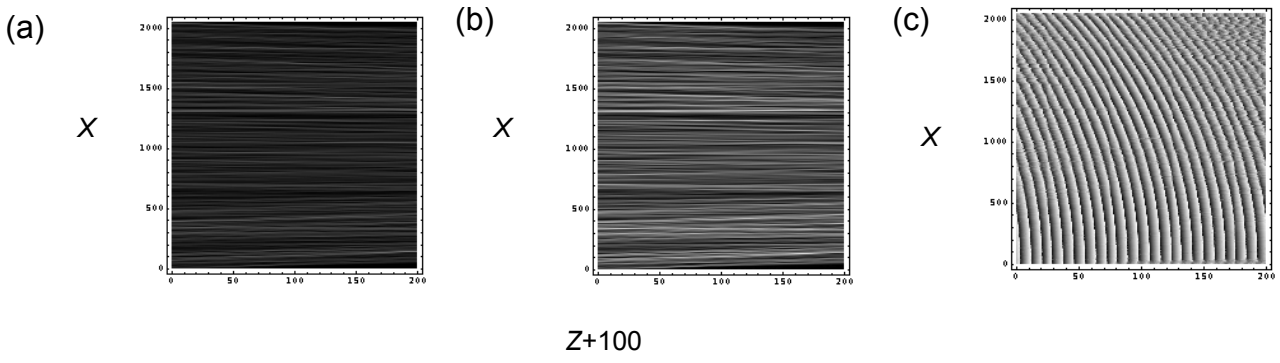

Fig. 9: Cross-sections of the reconstructed intensity at one wavelength (a), the phase (b) and the modulus (c) of the coherence factor, obtained from the dual wavelengths contouring. *X*-scale=6.7 μm, *Z*-scale=0.1 mm

applying an interferometric technique, for example, the dual wavelength method that can also be used for a uniform rough surface without any marking as mentioned above. We performed its numerical simulations

We employed the same object as in the previous section, a cylinder of 30 mm-diameter. Other parameters such as the object distance and the CCD specifications are the same as in the above simulations with target images. The wavelength shift of $\Delta\lambda$=0.5 nm was provided from the initial wavelength λ=660 nm. In Fig.9 we present the contours of the reconstructed intensity (a), and those of the magnitude (b) and phase (c) of the coherence factor.

The cross-section of the image intensity reconstructed with the same wavelength as in the hologram recording exhibits the uniform speckled appearance as shown in Fig.9 (a) because no marking is printed on the surface. Consequently smoothing of the intensity leads simply to a uniform image intensity distribution.

We see that the phase of the coherence factor that was calculated by averaging over 3 pixels (J=1) represents the shape of the average surface of the object , while its modulus varies more slowly in space. We notice the much higher sensitivity of the dual wavelength contouring from much narrower period of the phase contours than the focal depth of Fig.8(b).

Discussions and Conclusions

We have discussed the contouring of rough surfaces by phase-shifting digital holography that allows larger measurement area than off-axis digital holography. After the basic principles and experimental results of surface contouring were described, the model and results of computer simulation have been reported. The present method of simulation allows us to analyze the general experimental conditions including general object shape and optical systems as well as recording parameters of holograms and their processing. The rough surface can be uniform and/or have some marking on it

The effects of speckle noise on the measurement results have been discussed. For surfaces having some markings speckle suppression is necessary by smoothing the reconstructed intensity so that the marking image can be enhanced. In the case of uniform surface which can only be measured by the dual wavelength method with higher resolution phase of the coherence factor delivers surface height with better S/N than from the smoothed interferograms. The present quick advances in mega pixel digital cameras and rapid digital processors will proceed practical applications of the methods mentioned in this paper.

References

1. F. Cheng, G. M. Brown, and M. Song; “Ovweview of three-dimensional shape measurement using optical methods,”Opt. Eng. **39**(2000),10-22
2. I. Yamaguchi and T. Zhang; "Phase-shifting digital holography," Opt. Lett., **22**(1997), 1268-1270.
3. I. Yamaguchi, T. Ida, and M. Yokota; “Measurement of surface shape and position by phase-shifting Holography J. Holography Speckle, **3** (2006) 98-105.
4. I. Yamaguchi, T. Ida, M. Yokota, and K. Yamashita; “Surface shape measurement by phase-shifting digital holography with a wavelemgth shift,” Appl. Opt. 45(2006) 7610-7616.
5. I. Yamaguchi. and M. Yokota; ”Speckle noise suppression in measurement by phase-shifting digital holography,” *Opt. Eng*. **48**(2009), pp.085602-1-6.
6. I. Yamaguchi; “Holography. speckle, and computers”, Opt. Lasers in Eng. **39**(2003) 411-429.
7. I. Yamaguchi; ”Holography and speckle in phase-shifting digital holography”, *Chinese Optics Letters*, **7**(2009), pp 1104-1108.